Trop J Nat Prod Res, December 2025; 9(12): 5945 – 5954
ISSN 2616-0684 (Print)
ISSN 2616-0692 (Electronic)

Tropical Journal of Natural Product Research

Available online at https://www.tjnpr.org

Original Research Article

Molecular Docking Study of Moringin against Inflammatory and Oxidative Stress-Related Targets: Insights into Its Immunomodulatory Potential

Rafiastiana Capritasari[1,2], Arif B. Setianto[2]*, Akrom Akrom[2], Sapto Yuliani[2], Ichwan R. Rais[2]

[1]*Pharmacy Diploma Program, Faculty of Health Sciences, Universitas Muhammadiyah Magelang, Indonesia*
[2]*Doctoral Study Program of Pharmacy Sciences, Faculty of Pharmacy, Universitas Ahmad Dahlan, Indonesia*

ARTICLE INFO

Article history:
Received 15 July 2025
Revised 06 November 2025
Accepted 25 November 2025
Published online 01 January 2026

ABSTRACT

Moringin, an isothiocyanate derived from *Moringa oleifera*, has demonstrated notable pharmacological properties, including antiinflammatory and antioxidant activities. This study aimed to assess the immunomodulatory potential of moringin through molecular docking analyses targeting key proteins involved in inflammatory and oxidative stress pathways, including IL-6, IL-12, Nrf2, NOS, TNF-α, AT1R, and ACE. The three-dimensional structures of the target proteins were retrieved from the Protein Data Bank. Molecular docking was carried out using AutoDock Tools 1.5.6, and the resulting interactions were visualized by BIOVIA Discovery Studio Visualizer 24.1. The evaluation encompassed binding affinity, interactions with active residues, as well as ADME and toxicity assessments conducted using SwissADME and ProTox. Moringin demonstrated stronger binding affinities, reflected by more negative values than the native ligands across several receptors, including IL-12, Nrf2, NOS, and ACE. Among these, the most favorable binding was observed with the NOS receptor (−6.18 ± 0.182 kcal/mol), suggesting a stable and potent interaction with this target. Furthermore, the ADME analysis revealed good bioavailability and the absence of toxicity toward major organs, including the liver, nervous system, and immune system. Moringin also fulfilled the Lipinski`s criteria (molecular weight <500 Da, <5 hydrogen bond donors, <10 hydrogen bond acceptors, a log P<5, <10 rotatable bonds, and TPSA <140 Å) indicating its potential as a pharmacologically active compound. Overall, Moringin appears to hold considerable potential as a natural immunomodulatory and antioxidant agent. Nevertheless, additional validation through *in vitro* and *in vivo* studies is essential to substantiate these findings.

Keywords: Moringin, Molecular docking, Oxidative stress, Immunomodulator, Inflammatory cytokines.

Introduction

The immune system is essential for defending the body against pathogenic challenges while preserving physiological homeostasis. When dysregulated, particularly through chronic inflammation and oxidative stress, it contributes significantly to the development of various chronic diseases, including autoimmune disorders, cardiovascular conditions, and metabolic syndrome.[1,2] At the core of these pathological processes are critical molecular mediators, particularly proinflammatory cytokines such as interleukin-6 (IL-6), interleukin-12 (IL-12), and tumor necrosis factor-alpha (TNF-α), alongside oxidative stress-related factors including nitric oxide synthase (NOS) and the transcription factor Nrf2.[3] In addition, elements of the renin–angiotensin system, especially angiotensin-converting enzyme (ACE) and the angiotensin II type 1 receptor (AT1R), are known to modulate both inflammatory responses and oxidative stress pathways.[4,5]

Corresponding author; Email: arif.setianto@pharm.uad.ac.id
Tel: +62 812 2742 516

Citation. Capritasari R , Setianto B A , Akrom , Yuliani S, Rais R I. Molecular Docking Study of Moringin against Inflammatory and Oxidative Stress-Related Targets: Insights into Its Immunomodulatory Potential. Trop J Nat Prod Res. 2025; 9(12): 5945 – 5954 https://doi.org/10.26538/tjnpr/v9i12.6

Official Journal of Natural Product Research Group, Faculty of Pharmacy, University of Benin, Benin City, Nigeria.

Moringa oleifera, a plant widely recognized for its rich phytochemical profile and ethnopharmacological relevance has garnered significant attention for its therapeutic potential. One of the most notable bioactive compounds of *Moringa oleifera* is Moringin, an isothiocyanate produced through the enzymatic hydrolysis of glucomoringin. Emerging preclinical studies have highlighted its anti-inflammatory, antioxidant, and immunomodulatory properties.[6,7] Despite these encouraging findings, the precise molecular interactions between Moringin and immune-related target proteins is yet to be fully characterized. Accordingly, this study seeks to investigate the immunomodulatory potential of Moringin through *in silico* molecular docking analysis involving seven key protein targets associated by inflammation and oxidative stress: IL-6, IL-12, TNF-α, NOS, Nrf2, ACE, and AT1R. The findings are expected to offer meaningful computational insights into the multi-target mechanisms of Moringin and contribute to its prospective development as a natural immunomodulatory agent.

Materials and Methods

Computational tools

The computational analyses were performed on a laptop equipped with an Intel Dual Core N2840 processor. The software employed included VegaZZ version 2.4.0 (VEGA Software, 2015), AutoDock Tools version 1.5.6 (The Scripps Research Institute, 2019), BIOVIA Discovery Studio version 24.1 (Dassault System, 2023), and PyMOL version 2.3.3 (Schrodinger, LLC, 2019). The primary material consisted of the two-dimensional (2D) structure of the test compound, Moringin, that was constructed and geometrically optimized using

ISSN 2616-0684 (Print)
ISSN 2616-0692 (Electronic)

VegaZZ. Meanwhile, the crystallized structures of the target macromolecules - IL-6, IL-12, Nrf2, NOS, TNF-α, AT1R, and ACE were obtained from the Protein Data Bank (PDB).[8]

Molecular docking procedures
A molecular docking study was carried out to predict the binding interactions between Moringin and selected protein targets associated with inflammation and oxidative stress.

Ligand and protein preparation
The two-dimensional (2D) structure of Moringin was constructed and geometrically optimized using VegaZZ version 2.4.0. The optimized ligand was subsequently converted to a three-dimensional (3D) format and saved as a PDB file.
The 3D crystallographic structures of the selected target proteins IL-6 (1ALU)[9], IL-12 (6WDP)[10], NRF2 (4L7B)[11], NOS (3NOS)[12], TNF-α (7JRA)[13], AT1R (4ZUD)[14], and ACE (1O8A)[15] were downloaded from the Protein Data Bank. Protein preparation which included the removal of water molecules, the addition of polar hydrogen atoms, and the assignment of Kollman charges was performed using AutoDock Tools version 1.5.6. The processed proteins, along with the ligand, were subsequently converted into PDBQT format to enable docking analysis.

Molecular docking simulation
Molecular docking was conducted using AutoDock Vina, with a grid box positioned at the active site of each target protein. The grid dimensions were adjusted to ensure complete coverage of the binding pocket. The simulations generated multiple binding poses, and the conformation by the lowest binding energy (i.e., the most negative affinity) was selected for subsequent analysis.[16]

Data analysis
The docking outcomes, including binding affinities and molecular interactions, were visualized and analyzed using BIOVIA Discovery Studio Visualizer version 24.1 and PyMOL version 2.3.3. Key interactions, such as hydrogen bonding and hydrophobic contacts, were examined to elucidate the binding mechanisms between the ligand and receptor.[17]
Toxicity prediction was performed using the canonical SMILES representation of the test compound. Acute toxicity, expressed as LD_{50} values, was estimated using the ProTox web server.[18]

Results and Discussion

The molecular docking results were presented in the form of Root Mean Square Deviation (RMSD) values and binding affinities. The structures of the macromolecular targets analyzed in this study including IL-6 (1ALU), IL-12 (6WDP), Nrf2 (4L7B), NOS (3NOS), TNF-α (7JRA), AT1R (4ZUD), and ACE (1O8A) are presented in Figure 1. These protein structures were refined by isolating them from residual ligands and other non-relevant molecules to avoid potential interference with the ligand–receptor interaction process.[19] Hydrogen atoms were incorporated using AutoDock Tools to simulate the receptor structure more accurately under physiological conditions. This step was crucial, as the addition of hydrogen atoms helps approximate a pH close to 7, thereby reflecting the natural environment of the human body. [20]
Subsequently, structure optimization and grid box parameterization were performed. Redocking was then carried out using RMSD as a validation parameter. A redocking was considered successful when the RMSD value was below 2 Å, whereas values above this threshold indicate that the docking protocol and grid parameters were not suitable for generating reliable ligand-receptor binding predictions.[21]
The final stage of the procedure consisted of molecular docking, where each test ligand and reference compound were docked to its corresponding target receptor.
Table 1 presents the grid box coordinates and dimensions applied in the molecular docking process for each target protein. The grid box dimensions (X, Y, Z) were uniformly set at 40 Å, ensuring a consistent search space across all docking simulations. The center coordinates (X, Y, Z) defined the midpoint of each grid box in three-dimensional space and were positioned to cover the active site or binding pocket of the respective receptor. This configuration was critical, as the grid box

Table 1: Gridbox coordinate

PDB	Receptor	Gridbox					
		Dimension (Å)			Center		
		X	Y	Z	X	Y	Z
1ALU	IL-6	40	40	40	-7.677	-12.743	0.007
6WDP	IL-12	40	40	40	-26.706	-5.589	38.603
4L7B	Nrf2	40	40	40	27.905	-12.705	-0.01
3NOS	NOS	40	40	40	24.125	14.511	23.561
7JRA	TNF-α	40	40	40	-15.168	-2.292	-26.697
4ZUD	AT1R	40	40	40	-41.3	63.09	28.37
1O8A	ACE	40	40	40	38.647	22.113	68.485

Table 2: Root Mean Square Deviation (RMSD) Values

PDB	Receptor	RMSD
1ALU	IL-6	1.177±0.040
6WDP	IL-12	1.090±0.130
4L7B	Nrf2	0.000±0.000
3NOS	NOS	1.798±0.000
7JRA	TNF-α	0.467±0.733
4ZUD	AT1R	1.857±0.356
1O8A	ACE	0.279±0.028

Values are mean ± standard deviation (SD), n = 3

ISSN 2616-0684 (Print)
ISSN 2616-0692 (Electronic)

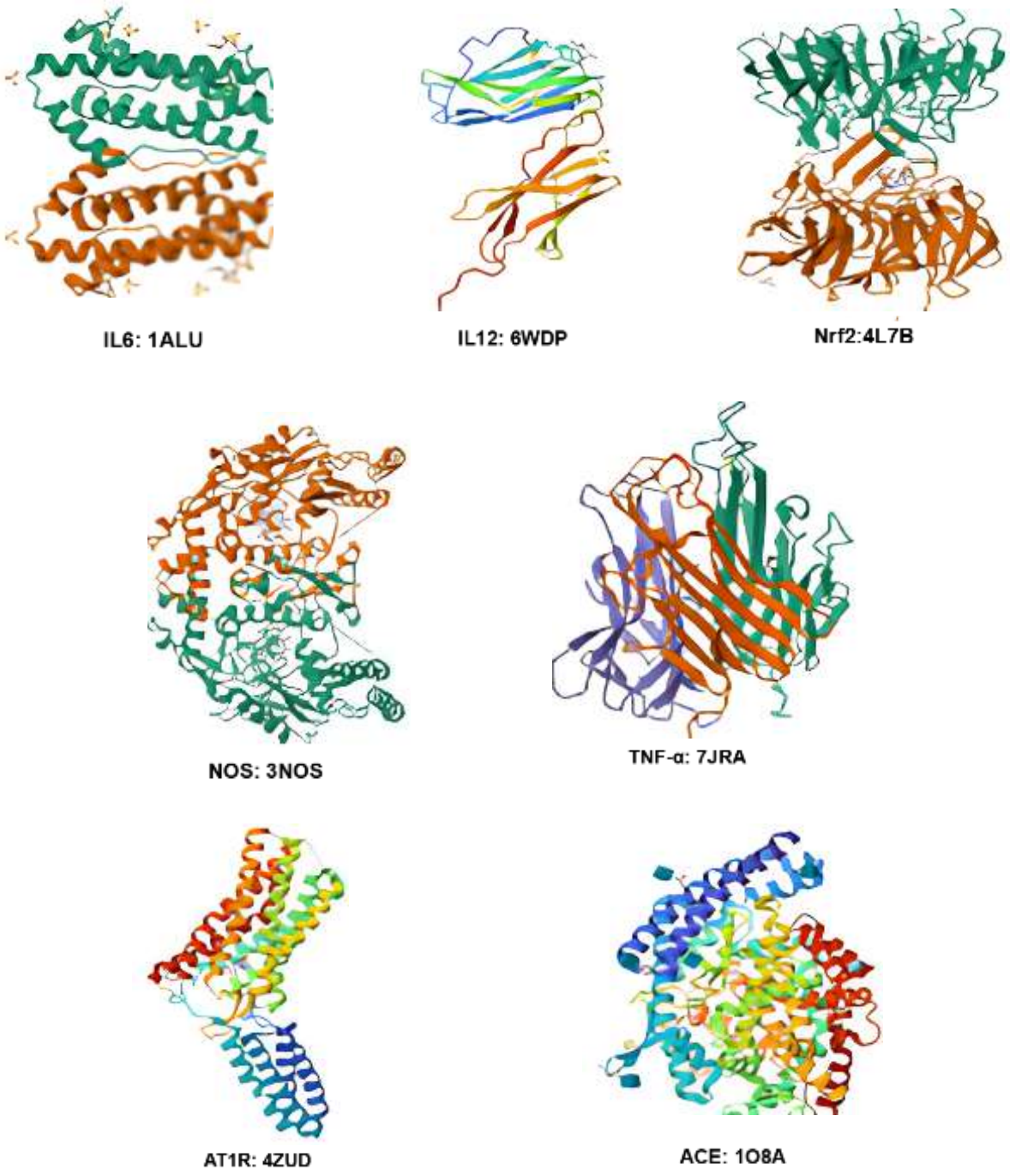

Figure 1: Structures of the target receptors

specifies the region where the docking program explores potential ligand–receptor interactions.

Table 2 presents the redocking results, assessed based on Root Mean Square Deviation (RMSD) values obtained from three replications (n = 3). An RMSD value below 2 Å was considered indicative of a valid docking method and grid box configuration, as it demonstrates the ability to reliably reproduce the original binding pose of the co-crystallized ligand. The RMSD values and interpretations are as follows: 1ALU (IL-6): 1.177 ± 0.040 Å (valid); 6WDP (IL-12): 1.099 ± 0.130 Å (valid); 4L7B (Nrf2): 0.000 ± 000 Å (excellent, no deviation, likely due to the ligand being in its native pose); 3NOS (NOS): 1.798 ± 000 Å (valid, approaching the threshold); 7JRA (TNF-α): 0.467 ± 0.733 Å (excellent); 4ZUD (AT_1R): 1.857 ± 0.356 Å (valid, near the upper limit) and 1O8A (ACE): 0.279 ± 0.028 Å (highly valid). All target proteins produced RMSD values below 2 Å, confirming that the grid box configuration and docking protocol were valid and reliable for the molecular docking of Moringin. Figure 2 presents an overlay of the native ligand poses before and after redocking, demonstrating the close alignment achieved during validation.

Subsequently, the test ligand Moringin was docked to the macromolecules IL-6, IL-12, Nrf2, NOS, TNF-α, AT1R, and ACE using AutoDock version 1.5.6 to evaluate its potential interactions. This procedure involved loading the validated grid parameters, the test ligand, and the target proteins. Docking was executed 100 times by three independent repetitions, with input files saved in .dpf format and output files generated in .dlg format.

ISSN 2616-0684 (Print)
ISSN 2616-0692 (Electronic)

The grid box settings applied in this step were identical to those used during the validation phase, ensuring consistent RMSD values and

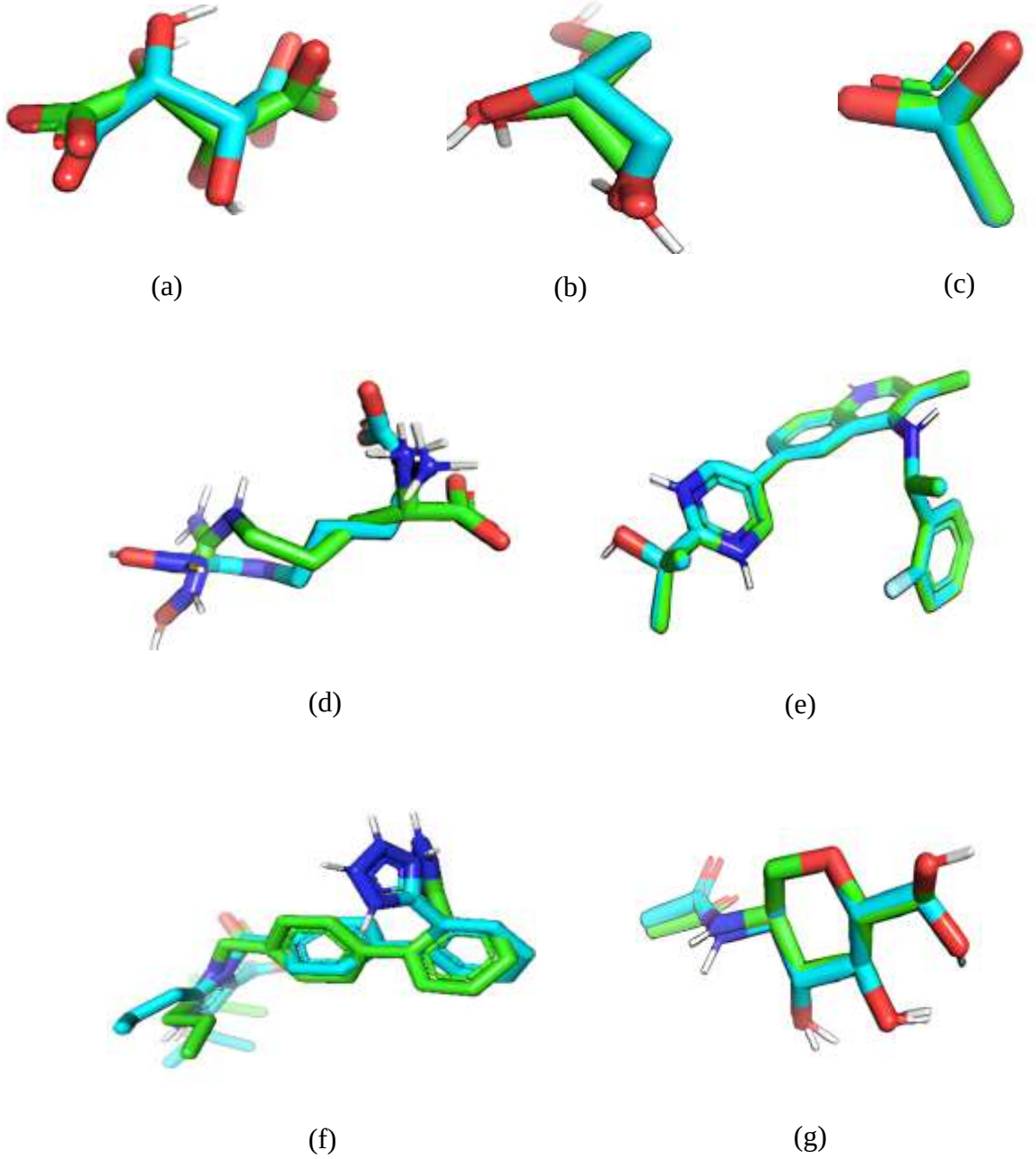

Figure 2: The 3D overlay visualization of native ligand. **a:** IL-6 (TLA); **b:** IL-12 (GOL); **c:** Nrf2 (ACT); **d:** NOS (HAR); **e:** TNF-α (VGY); **f:** AT1R (OLM), **g:** ACE (NAG)
before (green) and after (blue)

enhancing the reliability of the docking results. The analysis focused on binding free energy (ΔG_binding) and the characterization of interactions among the ligands and amino acid residues of each receptor. The resulting ligand conformations were ranked according to their ΔG_binding values, with lower (more negative) scores indicating more stable ligand–receptor complexes, while higher values reflected weaker interactions.[22]

Table 3 summarizes the amino acid residues of IL-6, IL-12, Nrf2, NOS, TNF-α, AT1R, and ACE that formed hydrogen bonds with Moringin. These interactions were primarily mediated by hydroxyl (–OH) and amine (–NH) functional groups, which play crucial role in stabilizing ligand–receptor binding. The results further indicate that Moringin exhibited more favorable binding affinities than the native ligands for several receptors, including IL-12, Nrf2, NOS, and ACE. The strongest affinity was observed with the NOS receptor (–6.18 ± 0.182 kcal/mol), suggesting a high potential for stable interaction at this target site. Conversely, in the case of the TNF-α receptor, the native ligand displayed the most favorable binding affinity among all complexes (–10.88 ± 0.061 kcal/mol), markedly exceeding that of Moringin.

In respect to inhibition constant (Ki) values, Moringin demonstrated stronger inhibitory potential (lower Ki values) than the native ligands, particularly at the Nrf2, NOS, and ACE receptors. On the NOS receptor, Moringin achieved a Ki of 42.22 μM, well below the 100 μM threshold, indicating good inhibitory efficacy and promising biological activity. In contrast, the Ki value for Nrf2 (2041.26 μM) reflected

ISSN 2616-0684 (Print)
ISSN 2616-0692 (Electronic)

weak binding affinity, suggesting limited biological effectiveness compared to other targets. For IL-12 and TNF-α, Moringin exhibited higher Ki values than the native ligands, indicating reduced inhibitory potential. Specifically

Table 3: Hydrogen bonding interaction of amino acid residues on the receptor

Receptor	Compound (Native ligand – Moringin)	Parameter		
		Binding affinity (kcal/mol±SD)	Inhibition constant (µm)	Amino acid residue
IL-6	TLA	-5.830±0.017	53.27	Arg179, Arg182, Gln175
	Moringin	-5.140±0.015	206.61	Ser176, Glu175, Arg182, Arg30, Asp26
IL-12	GOL	-2.140±0.060	27046.67	Glu153
	Moringin	-4.780±0.073	312.736	Gln154, Leu200, Glu201
Nrf2	ACT	-3.190±0.000	4610	Glu493
	Moringin	-5.033±0.011	204.216	Asn469, Arg494
NOS	HAR	-4.440±0.266	469.693	Gln247, Tyr357, Asn366
	Moringin	-6.180±0.182	42.22	Pro334, Gly355, Glu361
TNF-α	VGY	-10.880±0.061	0.010	Leu233, Tyr227, Tyr195
	Moringin	-5.740±0.005	61.886	Leu233, Tyr195
AT1R	OLM	-9.200±0.050	0.17	Tyr35
	Moringin	-6.620±0.015	13.986	Tyr87, Cys180, Arg167, Ile288
ACE	NAG	-3.770±0.047	1720	Thr74
	Moringin	-3.890±0.145	1416.67	Thr75, Glu76, Ile73

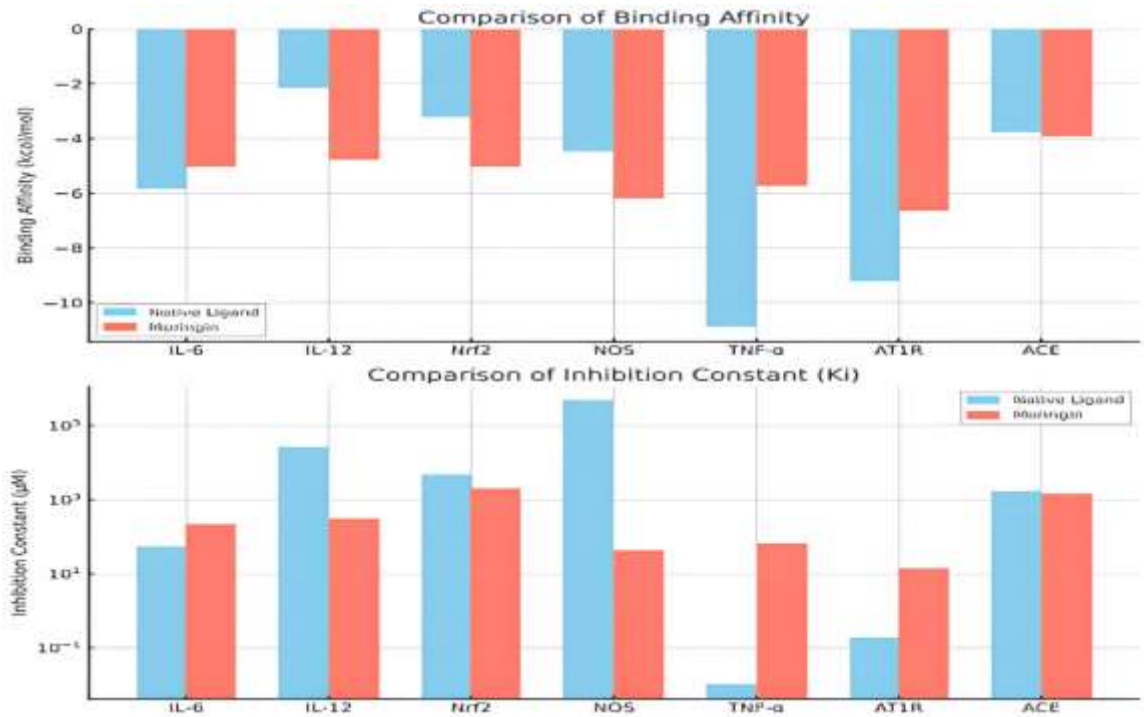

Figure 3: Comparative analysis of binding affinity (ΔG binding) and inhibition constanta (Ki) between native ligands and Moringin across multiple inflammatory and oxidative stress-related receptors (IL-6, IL-12, Nrf2, NOS, TNF-α, AT1R, ACE)

ISSN 2616-0684 (Print)
ISSN 2616-0692 (Electronic)

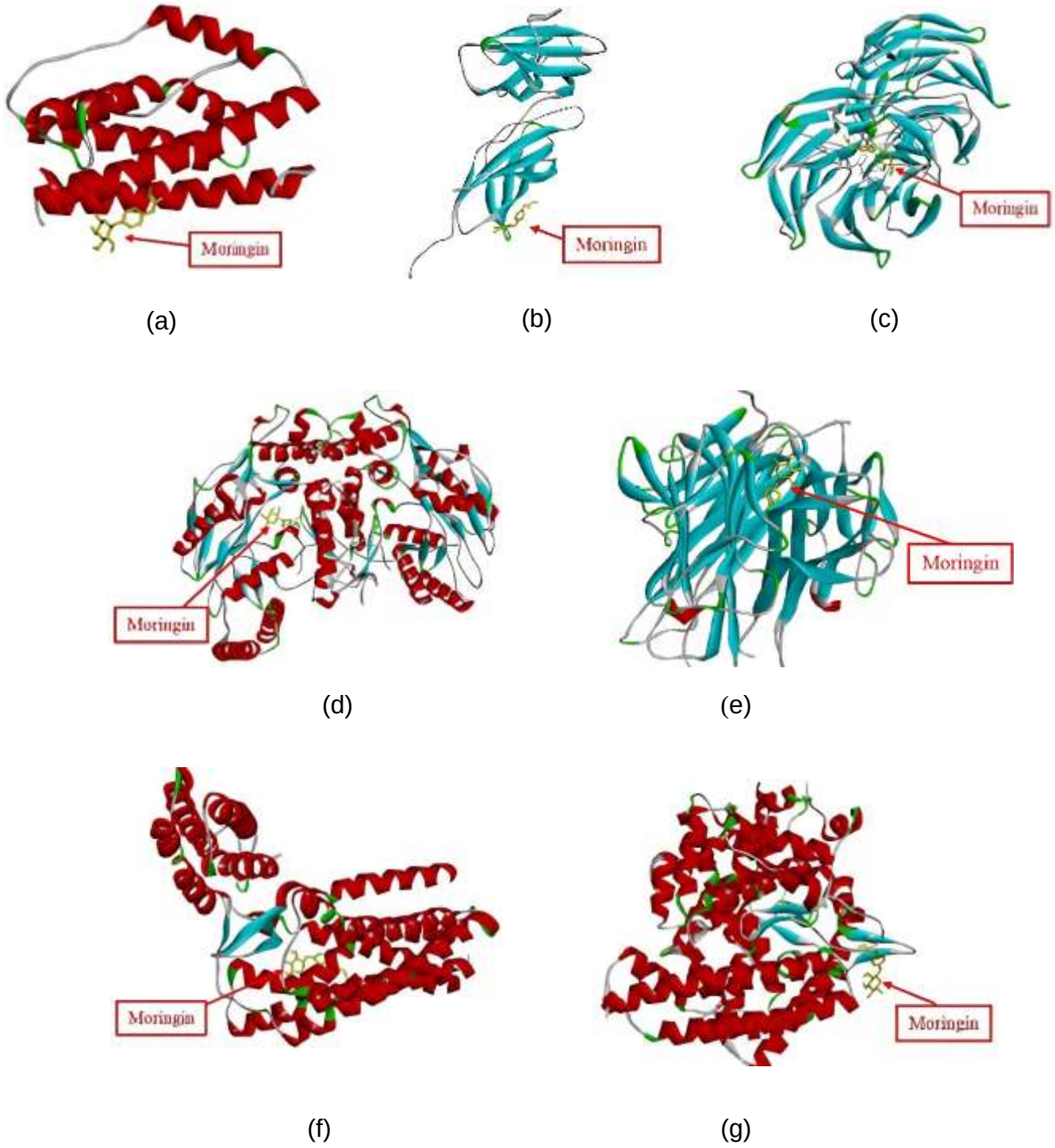

Figure 4: Visualization of the interaction between moringin and each macromolecule. **a:** IL-6-Moringin; **b:** IL-12-Moringin; **c:** Nrf2-Moringin; **d:** NOS-Moringin; **e:** TNF-α-Moringin; **f:** AT1R-Moringin, **g:** ACE-Moringin

ISSN 2616-0684 (Print)
ISSN 2616-0692 (Electronic)

Table 4: Similarity of amino acid residues and interaction distances between the receptor and the native ligand – moringin

Receptor	Similarity of amino acid residues	Interaction distance (Å)	
		Native ligand	Moringin
IL-6	Arg182,	2.74; 2.79	2.66
	Gln175	2.80	2.33
IL-12	-	-	-
Nrf2	-	-	-
NOS	Glu361	2.94	1.86; 2.13
TNF-α	Tyr195,	4.80	2.04
	Leu133	4.97; 4.73	5.16
AT1R	Trp84,	4.36	4.09
	Val108	4.40; 4.47	4.83
ACE	-	-	-

Table 5: Physicochemical and pharmacokinetic profiles of moringin

Parameter	Result
Physicochemical	
Molecular weight (< 500 Da)	311.35
Hydrogen bond donors (< 5)	3
Hydrogen bond acceptors (< 10)	6
MLogP (< 5)	0.99
Rotable bonds (< 10)	4
TPSA (< 140 Å)	123.60
Pharmacokinetic	
GI Absorption	High
BBB permeant	No
CYP1A2 inhibitor	No
CYP2C19 inhibitor	No
CYP2C9 inhibitor	No
CYP2D6 inhibitor	No
CYP3A4 inhibitor	No

IL-12 (312.736 μM) and AT1R (13.986 μM) revealed relatively high Ki values for Moringin, pointing to weaker inhibition, though still within the range of possible biological relevance.

The number and type of hydrogen bonds offer valuable insights into the specificity and stability of ligand–receptor interactions. Moringin was found to form multiple hydrogen bonds with active site residues across nearly all receptors. For example, in IL-6, Moringin interacted with Ser176, Glu175, and Arg182, which differred from the interaction profile of the native ligand. In IL-12 docking, the native ligand established only one hydrogen bond with Glu153, while Moringin formed three hydrogen bonds with Glu153, Leu200, and Glu201. A similar trend was observed for Nrf2, where the native ligand formed a single hydrogen bond with Glu493, while Moringin engaged in three hydrogen bonds involving Asn469, Arg494, and Glu493. These additional interactions suggest that Moringin established stronger and more complex binding with IL-12 and Nrf2, consistent with its more favorable binding affinity compared to the native ligands.

In the docking analysis with NOS, both Moringin and the native ligand formed five hydrogen bonds, though they interacted through different residues. The native ligand interacted with Gln357, Asn366, Glu361, and Trp356, while Moringin bounded to Pro334, Gly355, Glu361, Trp447, and Arg183. Notably, Glu361 served as a common interaction site for both ligands, suggesting it may represent a conserved and critical residue in the ligand–receptor binding interface. For TNF-α, the native ligand formed three hydrogen bonds with Leu233, Tyr227, and Tyr195, while Moringin established only two hydrogen bonds, involving Leu233 and Tyr195. This reduction in hydrogen bonding corresponds with the lower binding affinity observed for Moringin at this receptor. Because hydrogen bonds are closely associated with binding strength, fewer interactions typically result in less stable ligand–receptor complexes. Strong hydrogen bonding not only enhances binding affinity but can also influence key physicochemical properties, including solubility and boiling point. [23]

For AT1R, the native ligand formed a single hydrogen bond with Tyr35, while Moringin established four hydrogen bonds with Tyr35, Cys180, Arg167, and Ile288. Despite this greater number of interactions, Moringin displayed lower binding affinity than the native ligand, likely due to suboptimal bond geometry or positioning. A comparable pattern was observed with ACE, where Moringin formed hydrogen bonds with Thr74, Glu76, and Ile73, while the native ligand interacted solely with Thr74. Nevertheless, the binding affinity of Moringin remained lower, indicating that the number of hydrogen bonds alone does not necessarily correspond to stronger binding. Binding affinity is influenced not only by the quantity of hydrogen bonds but also by their quality and spatial orientation, together with

ISSN 2616-0684 (Print)
ISSN 2616-0692 (Electronic)

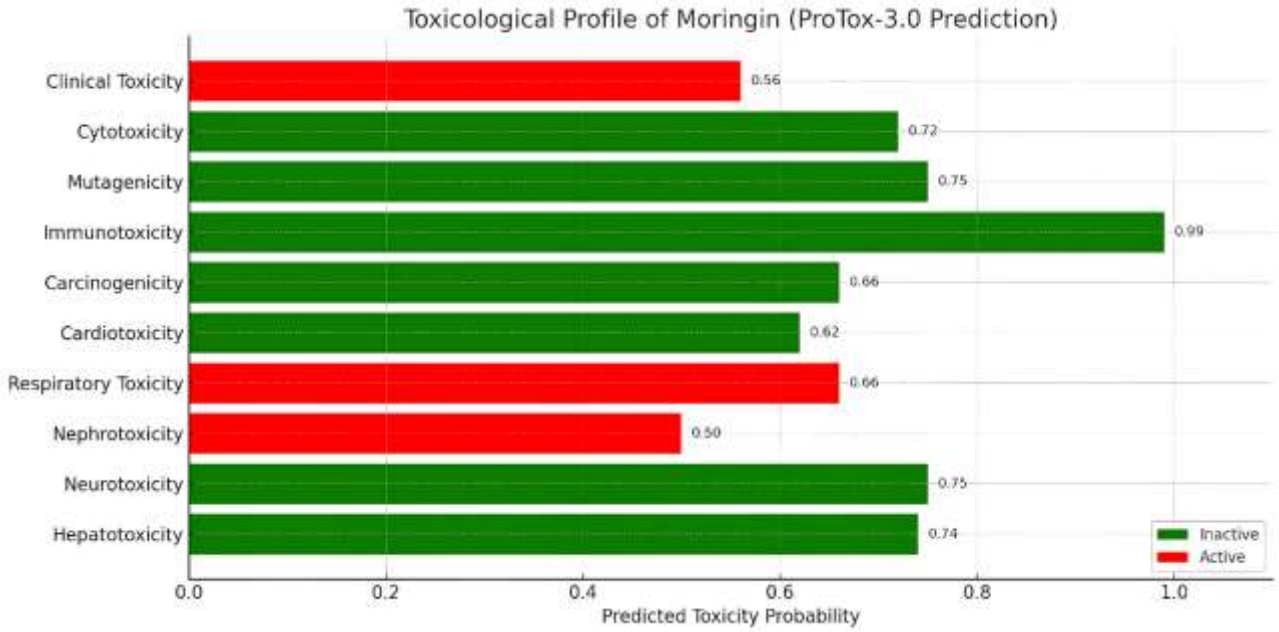

Figure 5: Toxicological profile of moringin
Green (inactive): Does not show potential toxicity
Red (Active): Potential toxicity detected (requires attention)

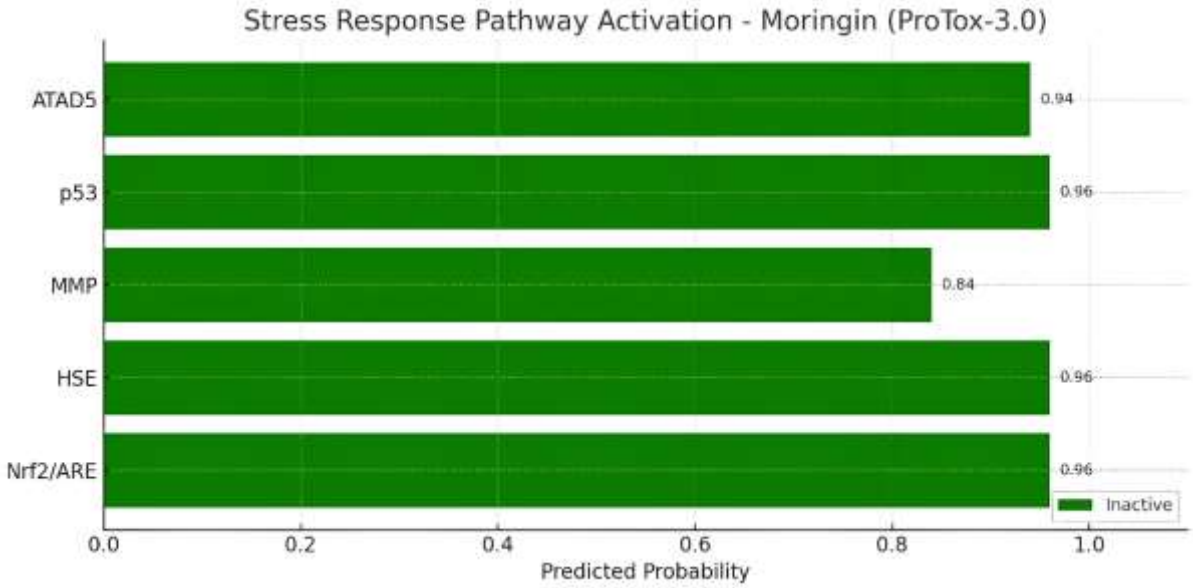

Figure 6: Stress response pathway activation by moringin

additional factors such as hydrophobic, electrostatic, and π–π interactions, molecular flexibility, entropic effects, solvent influence (e.g., water), and the structural environment of the active site. [24]

Moringin demonstrates notable immunomodulatory and antioxidant potential through its interactions with several key targets, particularly Nrf2 and NOS, as reflected in its binding affinities and inhibition constants. Conversely, for certain targets such as TNF-α and IL-12, its effectiveness appears lower than that of the native ligands. The presence of multiple hydrogen bond interactions indicates a degree of complex stability, further reinforcing the potential of moringin as a promising bioactive compound.

Moringin exhibited competitive or, in some cases, superior binding affinities compared to the native ligands, particularly with NOS and Nrf2. Its inhibition constant (Ki) values were generally lower, reflecting stronger inhibitory potential, except for TNF-α and AT1R, where the native ligands revealed greater potency. For clarity, all inhibition constant values are presented on a logarithmic scale (Figure 3).

The interactions between moringin and its target macromolecules, represented as three-dimensional (3D) protein structures obtained through molecular docking, are illustrated in Figure 4. The visualization depicts the orientation and positioning of moringin in the respective binding sites, providing structural insight into its potential mechanisms of action. These docking results support the proposed pharmacological activities of moringin, including anti-inflammatory, antioxidant, and immunomodulatory effects. The selected protein targets, IL-6, IL-12, and TNF-α are pro-inflammatory cytokines which play central roles in the body's inflammatory response. Produced by immune cells in reaction to infection, injury, or other external stimuli, these cytokines orchestrate inflammation by recruiting additional immune cells and stimulating the production of inflammatory mediators.[25,26]

Nrf2 is a central regulator of the antioxidant response pathway, functioning to protect cells from oxidative damage. It governs the expression of antioxidant enzymes and other genes that contribute to cellular defense against oxidative stress. Typically, Nrf2 activation is initiated by stress signals such as reactive oxygen species (ROS), which in turn stimulate the upregulation of genes responsible for neutralizing ROS and detoxifying harmful compounds.[27,28]

Nitric oxide synthase (NOS) is an enzyme that generates nitric oxide (NO), a key signaling molecule involved in a wide range of physiological processes. NOS catalyzes the conversion of L-arginine to L-citrulline and NO. The NOS family comprises three isoforms, neuronal NOS (nNOS), endothelial NOS (eNOS), and inducible NOS (iNOS), each playing distinct roles across different tissues.[29] AT_1R and ACE are components of the renin-angiotensin system and are known to contribute to both inflammatory responses and oxidative stress.[30]

Table 4 summarizes the similarity of interacting amino acid residues along with their respective interaction distances. Residue similarity refers to cases where moringin interacts with the same residues as the native ligand. Interaction distance denotes the spatial separation among donor and acceptor atoms, with shorter distances, typically within the range of 1.8 – 3.0 Å, indicating a greater likelihood of hydrogen bond formation.[16,32]

Analysis of the IL-6 receptor indicates residue overlap at Arg182 and Gln175 for both the native ligand and moringin. Interestingly, the interaction distance at Gln175 was shorter in the moringin complex (2.23 Å vs. 2.66 Å), suggesting a stronger interaction at this critical residue. In contrast, for the IL-12 receptor, no common interacting residues were identified, implying that moringin binds at an alternative site. Nevertheless, moringin demonstrated a more favorable binding affinity (−4.78 ± 0.073 kcal/mol), that may have resulted from the formation of stable interactions at this novel binding site.

A similar observation was found with the Nrf2 receptor, where no overlapping residues were involved. Despite this observation, moringin exhibited a strong binding affinity (−5.03 ± 0.011 kcal/mol), suggesting the formation of stable interactions at a novel binding site. In the case of the NOS receptor, both ligands interacted with the critical residue Glu361. Notably, moringin formed shorter hydrogen bonds with Glu362 (1.86 Å and 2.13 Å) compared to the native ligand (2.94 Å), indicating a stronger interaction. This is consistent with its enhanced binding affinity (−6.18 ± 0.182 kcal/mol vs. −4.44 ± 0.266 kcal/mol).

For the TNF-α receptor, overlapping interactions were identified at Tyr195 and Leu133. Moringin established a much shorter hydrogen bond with Tyr195 (2.04 Å vs. 4.80 Å), suggesting a stronger localized interaction. Nevertheless, despite this favorable contact, moringin demonstrated a lower overall binding affinity compared to the native ligand (−5.74 ± 0.005 kcal/mol vs. −10.88 ± 0.061 kcal/mol), indicating a less optimal overall binding profile.

For the AT1R receptor, interactions were also detected at Trp8 and Val108; however, the relatively long interaction distances (>4 Å) indicate hydrophobic contacts, which are typically weaker than hydrogen bonds. In the case of the ACE receptor, no overlapping residue interactions were observed, suggesting that moringin binds at an alternative site. Despite this difference, its binding affinity remained comparable to that of the native ligand (-3.89 ± 0.145 kcal/mol vs. -3.77 ± 0.047 kcal/mol), implying that the alternative binding site can still support a relatively stable interaction.

Although Moringa oleifera has shown promising *in silico* activity in inhibiting target proteins related to immunomodulatory functions, these findings require validation through *in vitro* and *in vivo* investigations. Furthermore, a thorough assessment of its physicochemical characteristics, pharmacokinetic behavior, and toxicity profile is necessary to provide a more comprehensive understanding of its therapeutic potential.

To address these considerations, the present study incorporated an *in silico* evaluation of the physicochemical properties, pharmacokinetic profile, and safety characteristics of moringin. Assessing physicochemical attributes is a crucial step in determining drug-likeness, as it encompasses parameters such as partition coefficient (Log P), molecular weight, hydrogen bond donors and acceptors, and molar refractivity. Collectively, these parameters are summarized in Lipinski's Rule of Five, that serves as a benchmark for predicting the potential of a compound as an orally active drug candidate.

According to Lipinski's rule, an ideal drug candidate generally possesses a molecular weight under 500 Da, no more than five hydrogen bond donors, no more than ten hydrogen bond acceptors, a log P value below 5, fewer than ten rotatable bonds, and a topological polar surface area (TPSA) of less than 140 Å.[16,33] This rule is widely recognized as a guideline for identifying compounds with favorable pharmacokinetic and physicochemical characteristics. In this study, moringin met all the criteria of Lipinski's Rule of Five (Table 5), reinforcing its potential as a promising lead compound for the development of immunomodulatory therapies.

Acute toxicity testing of the moringin compound revealed an LD_{50} value of 2500 mg/kg, placing it in Toxicity Class 5. The LD_{50} parameter is commonly used to assess the relative potency of compounds, where a lower LD_{50} indicates that even a small dose is sufficient to cause mortality in 50% of the test animals.[33] Moringin exhibited no predicted toxicity toward major organs, including the liver (hepatotoxicity), nervous system (neurotoxicity), and immune system (immunotoxicity), and it was also classified as non-carcinogenic (Figure 5).

Figure 6 presents the graph of cellular stress response pathway activation (Tox21) by moringin. According to predictions from ProTox-3.0, key pathways, including Nrf2/ARE (antioxidant and detoxification), p53 (DNA damage response), HSE (heat shock response), MMP (mitochondrial function), and ATAD5 (genome stability) were all predicted to remain inactive in the presence of moringin. These results, supported by a high probability value (>0.9), provide strong evidence that moringin does not induce oxidative stress, genotoxicity, or mitochondrial damage.

Conclusion

This *in silico* investigation highlights the potential of moringin, an isothiocyanate derived from *Moringa oleifera*, as both an immunomodulatory and antioxidant agent. Molecular docking analyses against seven key targets associated with inflammatory and oxidative stress pathways (IL-6, IL-12, TNF-α, Nrf2, NOS, AT1R, and ACE) revealed that moringin exhibited strong binding affinity, particularly with NOS and Nrf2. Furthermore, moringin established multiple stable hydrogen bonds and engaged in specific interactions with the active site amino acid residues of these targets, thereby reinforcing its potential as an effective biological ligand. Additionally, moringin satisfied Lipinski's Rule of Five and demonstrated a favorable pharmacokinetic profile, including good intestinal absorption, while exhibiting no toxicity toward major organs. Nevertheless, interactions with several targets, such as TNF-α and IL-12, suggest that its effectiveness remains lower than that of the native ligand. Hence, further *in vitro* and *in vivo* investigations are required to validate these *in silico* findings and to provide a more comprehensive evaluation of moringin's therapeutic potential.

Conflict of Interest

The authors declare no conflict of interest.

Authors' Declaration

The authors hereby declare that the work presented in this article is original and that any liability for claims relating to the content of this article will be borne by them.

Acknowledgments

This research was supported financially by the Directorate of Research, Technology, and Community Services, Ministry of Education, Culture, Research, and Technology of Indonesia, under Grant No. 107/E5/PG.02.00.PL/2024; 0690.12/LL5-INT/AL.04/2024; and 018/PFR/LPPUAD/VI/2024.

References

Therapeutic Implications. Signal Transduct Target Ther. 2025; 10(1):166.
2. Blanco LP and Kaplan MJ. Metabolic Alterations of the Immune System in the Pathogenesis of Autoimmune Diseases. PLoS Biol. 2023; 21(4):1–13.
3. Zhang H and Dhalla NS. The Role of Pro-Inflammatory Cytokines in the Pathogenesis of Cardiovascular Disease. Int J Mol Sci. 2024; 25(2):1082.
4. Silva GM, França-Falcão MS, Calzerra NTM, Luz MS, Gadelha DDA, Balarini CM. Role of Renin-Angiotensin System Components in Atherosclerosis: Focus on Ang-II, ACE2, and Ang-1–7. Front Physiol. 2020; 11(1067):3–10.
5. Tomasik AM and PJ. A New Perspective on the Renin-Angiotensin System. Diagnostics 2023; 13(16):1–12.
6. Pareek A, Pant M, Gupta MM, Kashania P, Ratan Y, Jain V. *Moringa oleifera*: An Updated Comprehensive Review of Its Pharmacological Activities, Ethnomedicinal, Phytopharmaceutical Formulation, Clinical, Phytochemical, and Toxicological Aspects. Int J Mol Sci. 2023; 24(2089):1-36.
7. Lopez-Rodriguez NA, Gaytán-Martínez M, de la Luz Reyes-Vega M, Loarca-Piña G. Glucosinolates and Isothiocyanates From *Moringa oleifera*: Chemical and Biological Approaches. Plant Foods Hum Nutr. 2020; 75(4):447–457.
8. Zhang H, Unal H, Desnoyer R, Han GW, Patel N, Katritch V. Structural Basis for Ligand Recognition and Functional Selectivity at Angiotensin Receptor. J Biol Chem. 2015; 290(49):29127–29139.
9. Salman HA, Yaakop AS, Aladaileh S, Mustafa M, Gharaibeh M, Kahar UM. Inhibitory Effects of *Ephedra alte* on IL-6, Hybrid TLR4, TNF-α, IL-1β, and Extracted TLR4 Receptors: In Silico Molecular Docking. Heliyon. 2023; 9(1):1-9.
10. Glassman CR, Mathiharan YK, Jude KM, Su L, Panova O, Lupardus PJ. Structural Basis for IL-12 and IL-23 Receptor Sharing Reveals a Gateway for Shaping Actions on T Versus NK Cells. Cell. 2021; 184(4):900-914.
11. Prasetiawati R, Febrianti EN, Hamdani S, Ikram NKK, Fakih TM, Novitasari D. Alpha-Mangostin From *Garcinia mangostana* L.: A Potential Nrf2 Inhibitor for Long COVID-19 Explored Through Molecular Dynamics. J Pharm Pharmacogn Res. 2025; 13(2):381–392.
12. Madariaga-Mazõn A, Hernández-Abreu O, Estrada-Soto S, Mata R. Insights on the Vasorelaxant Mode of Action of Malbrancheamide. J Pharm Pharmacol. 2015; 67(4):551–558.
13. Velmurugan Y, Chakkarapani N, Natarajan SR, Jayaraman S, Madhukar H, Venkatachalam R. PPI Networking, *In-Vitro* Expression Analysis, Virtual Screening, DFT, and Molecular Dynamics for Identifying Natural TNF-α Inhibitors for Rheumatoid Arthritis. Mol Divers. 2025.
14. Xu Y, Al-Mualm M, Terefe EM, Shamsutdinova MI, Opulencia MJC, Alsaikhan F. Prediction of COVID-19 Manipulation by Selective ACE Inhibitory Compounds of *Potentilla reptans* Root: In Silico Study and ADMET Profile. Arab J Chem. 2022; 15(7):103942.
15. Natesh R, Schwager SLU, Sturrock ED, Acharya KR. Crystal Structure of the Human Angiotensin-Converting Enzyme-Lisinopril Complex. Nature. 2003; 42:551–554.
16. Nur S, Hanafi M, Setiawan H, Nursamsiar N, Elya B. Molecular Docking Simulation of Reported Phytochemical Compounds from *Curculigo latifolia* Extract on Target Proteins Related to Skin Antiaging. Trop J Nat Prod Res. 2023; 7(11):5067–5080.
1. Wang X, Chen L, Wei J, Zheng H, Zhou N, Xu X. The Immune System in Cardiovascular Diseases: From Basic Mechanisms to
17. Ferwadi S, Rahmat G, Astuti W. Molecular Docking Study of Cinnamate Acid Compound and its Derivatives as Protein 1J4X Inhibitor to Cervical Cancer Cell. J Kim Mulawarman. 2017; 14(2):84–90.
18. Ruswanto, Siswandono, Richa M, Tita N, Tresna L. Molecular Docking of 1-Benzoyl-3-Methylthiourea as Anti Cancer Candidate and its Absorption, Distribution, and Toxicity Prediction. J Pharm Sci Res. 2017; 9(5):680–684.
19. Shakil S. A Simple Click by Click Protocol to Perform Docking: Autodock 4.2 Made Easy for Non-Bioinformaticians. Excli J. 2013; 12:831–857.
20. Shamsi A, Khan MS, Yadav DK, Shahwan M, Furkan M, Khan RH. Structure-Based Drug-Development Study Against Fibroblast Growth Factor Receptor 2: Molecular Docking and Molecular Dynamics Simulation Approaches. Sci Rep. 2024; 14(1):1–13.
21. Allouche A. A Graphical User Interface for Computational Chemistry Softwares. J Comput Chem. 2012; 32:174–182.
22. Umamaheswari M, Madeswaran A, Asokkumar K. Virtual Screening Analysis and In-Vitro Xanthine Oxidase Inhibitory Activity of Some Commercially Available Flavonoids. Iran J Pharm Res. 2013; 12(3):317–323.
23. Dong K, Zhang S, Wang J. Understanding the Hydrogen Bonds in Ionic Liquids and Their Roles in Properties and Reactions. Chem Commun. 2016; 52(41):6–23.
24. Qing R, Hao S, Smorodina E, Jin D, Zalevsky A, Zhang S. Protein Design: From the Aspect of Water Solubility and Stability. Chem Rev. 2022; 122:14085–14179.
25. Elgellaie A, Thomas SJ, Kaelle J, Bartschi J, Larkin T. Pro-Inflammatory Cytokines IL-1α, IL-6 and TNF-α in Major Depressive Disorder: Sex-Specific Associations with Psychological Symptoms. Eur J Neurosci. 2023; 57(11):1913–1928.
26. Zhang JM and An J. Cytokines, Inflammation and Pain. Int Anesth Clin. 2007; 45(2):27-37.
27. Fujiki T, Ando F, Murakami K, Isobe K, Mori T, Susa K. Tolvaptan Activates the Nrf2/HO-1 Antioxidant Pathway Through PERK Phosphorylation. Sci Rep. 2019; 9(1):1–10.
28. Singh S, Nagalakshmi D, Sharma KK, Ravichandiran V. Natural Antioxidants for Neuroinflammatory Disorders and Possible Involvement of Nrf2 Pathway: A Review. Heliyon. 2021; 7(2):1-10.
29. Dong S, Lyu X, Yuan S, Wang S, Li W, Chen Z. Oxidative Stress: A Critical Hint in Ionizing Radiation Induced Pyroptosis. Radiat Med Protect. 2020; 1(4):179–185.
30. Jackson L, Eldahshan W, Fagan SC, Ergul A. Within the Brain: The Renin Angiotensin System. Int J Mol Sci. 2018; 19(3):1–23.
31. Öztürk H, Ozkirimli E, Özgür A. A comparative study of SMILES-based compound similarity functions for drug-target interaction prediction. BMC Bioinformatics 2016;17(1):1–11.
32. Kristianti MTF, Goenawan H, Achadiyani A, Sylviana N, Lesmana R. The Potential Role of Vitamin D Administration in The Skin Aging Process Through The Inflammatory Pathway: A Systematic Review. Trop J Nat Prod Res. 2023;7(4):2675–81.
33. Morris-Schaffer K, McCoy MJ. A Review of the LD50and Its Current Role in Hazard Communication. ACS Chem Heal Saf. 2021;28(1):25–33.